

Preparation of Carbon-Coated Cobalt Nanocrystals in a New Gas Blow Arc Reactor and Their Characterization

Houjin Huang,[†] Shihe Yang,^{*,†} and Gang Gu^{†,‡,§}

Department of Chemistry, Hong Kong University of Science & Technology, Clear Water Bay, Kowloon, Hong Kong, and Department of Physics, Nanjing University, Nanjing, P. R. China

Received: December 16, 1997; In Final Form: February 19, 1998

Carbon-coated cobalt nanocrystals were prepared by a modified method of arc discharge under a He gas blow around a graphite rod cathode. The morphology and structure of the carbon coating and the cobalt enclosure were examined by high-resolution transmission electron microscopy, Raman scattering, and X-ray diffraction. The magnetic properties of these particles after acid treatment were measured with a vibrating sample magnetometer and a thermogravimetric analyzer in a magnetic field gradient. Typical sizes of these particles were 20–40 nm depending on the discharge conditions. Large shifts of Raman peaks were observed upon acid treatment, reflecting the structural change of the carbon shell induced by the acid treatment. The blocking temperature of the sample was estimated to be 373 °C.

Introduction

Encapsulation of ferromagnetic metals within nanoscale carbon cages has attracted much attention in recent years, because of the interesting properties of these nanostructured ferromagnetic materials and their potential applications as high-density magnetic recording media, ferrofluids, and magnetic resonance imaging agents.^{1–6} One of the most desirable features of these materials is that the protective graphite coating markedly enhances the stability of the ferromagnetic nanoparticles while retaining the bulk of the materials' ferromagnetic properties.

During the past few years, several versions of the arc-discharge method derived from the Krätschmer–Huffman procedure for the production of fullerenes have been developed to prepare carbon-coated nanoparticles. McHenry et al. generated carbon-coated Gd₂C₃ (ref 1) and Co (ref 2) nanoparticles by arc evaporating a mixed carbon rod with a low metal-to-carbon ratio (~0.04 molar ratio) under static gas conditions. The Co particles prepared by this method were 0.5–5 nm in radius and exhibited superparamagnetic response at room temperature with a blocking temperature (T_B) of 160 K. The problem with this method was the production of too much carbon debris including amorphous carbon, nanotubes, and fullerenes. Shortly thereafter, Saito et al. (ref 3) and Seraphin et al. (ref 4) raised the metal-to-carbon ratio (≥ 20 wt %) and obtained graphite-coated particles ranging in size from several to hundreds of nanometers. Dravid et al. further reduced the carbon debris by employing a high-speed jet of helium gas (20–56 m/s) orthogonal to the gap between the two electrodes and by replacing the graphite cathode with a tungsten rod.⁵ The nanoparticle size could be controlled simply by changing the helium jet velocity. Later, Jiao et al. demonstrated that the particle size can be controlled by varying the diameter of the anode crucible to adjust the carbon supply.⁴ On the basis of these improvements, a large number of elements have been trapped in carbon cages as nanocrystals.^{4,5}

The methods mentioned above are all based on a vertical configuration with the cathode mounted over the top of a metal-containing graphite anode crucible. The graphite crucible is used not only to provide a source of carbon but also to prevent the molten material from spilling out. One of the difficulties associated with this configuration is to keep the gas outlet directly against the moving discharge plasma, especially when the metals are consumed below the top edge of the graphite crucible. Moreover, in the above horizontal blowing method, because of the inhomogeneous and dynamic environment caused by the strong horizontal gas blow, different pathways for particle encapsulation may be activated, resulting in a greater structural variation in the final products.^{5,6}

In this work, we attempt to introduce the gas jet vertically around the graphite cathode into the arc-discharge gap to synthesize carbon-coated cobalt nanocrystals. There are three advantages of this modification. First, the cobalt and carbon species in the plasma region can be quenched more evenly since the gas can disperse the particles in all directions instead of only one direction as in the horizontal gas-blowing configuration. This is expected to result in the formation of more uniform nanoparticles. Second, the difficulty in aiming the helium jet exactly at the discharge plasma can be avoided, especially when the cobalt level goes below the edge of the crucible upon arc discharge. Third, much less gas is needed in comparison with the horizontal blowing method. The carbon-coated nanocrystals prepared by this method were examined by transmission electron microscopy (TEM), Raman scattering, and X-ray diffraction (XRD). The effects of acid treatment on the carbon shell were studied by Raman scattering. The blocking temperature (T_B) of our sample was found to be 373 °C with a thermogravimetric (TG) analyzer in a magnetic field gradient.

Experimental Procedure

The carbon-coated cobalt nanocrystal samples were prepared by using a newly modified Krätschmer–Huffman arc-discharge method. Unlike the horizontal jet configuration used by other groups (Figure 1a), a steady stream of helium gas was passed along the periphery of the graphite cathode and through the gap

* Corresponding author. E-mail: chsyang@usthk.ust.hk.

[†] Hong Kong University of Science & Technology.

[‡] Nanjing University.

[§] On leave from Nanjing University, P. R. China.

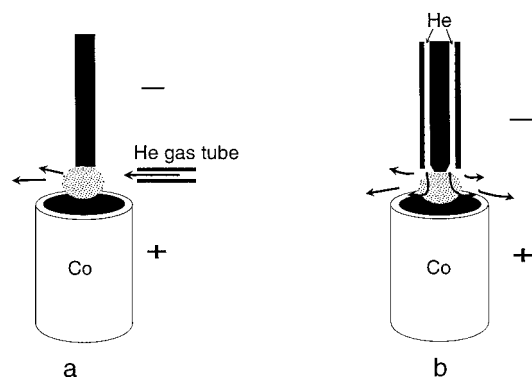


Figure 1. Schematic diagrams of the two types of modified Krätschmen-Huffman arc-discharge setups: traditional horizontal He-blowing scheme (a) and our modified version (b) used in the present study.

between the cathode and an outer graphite shell (Figure 1b). The inner cathode diameter was 4 mm, and the outer shell diameter was 12 mm. The width of the gap was 1.5 mm. The cathode protruded toward the anode by 2 mm relative to the outer graphite shell so as to facilitate particle dispersion. The anode was a 27-mm diameter graphite crucible with an inner diameter of 23 mm. This crucible was filled with molten cobalt. The flow rate of He gas was varied between 0.5 and 8 L/min, corresponding to the gas speeds of 0.32–5.2 m/s. For a typical arc discharge at a dc current of 120 A, a potential difference of 16 V, and a helium pressure of 250 Torr, 2–3 g of powder could be obtained in 15 min.

Part of the raw sample was immersed in 2 M HNO_3 under ultrasonic agitation for 15 min and then kept in the acid solution for 1 week or longer. The powder was transferred to the wall of the container by the application of a magnetic field and then washed with deionized water at least three times. Small amounts of the original and acid-treated powders were suspended in methanol after sonication for TEM experiments. Dried powder samples were also used for XRD, Raman scattering, and magnetic property measurements.

The powder samples were examined in a Phillips CM 20 TEM operated at 200 kV. Raman Scattering measurement was carried out in a Renishaw system (model 3000) using an Ar^+ laser beam at 514.5 nm. XRD experiments were conducted using a PW1830 (Phillips) X-ray diffractometer with the $\text{Cu K}\alpha$ radiation source. The magnetic hysteresis loop and the blocking temperature of the samples were measured by a vibrating sample magnetometer (VSM) and a thermogravimetric (TG) analyzer in a magnetic field gradient.

Results and Discussion

Figure 2a shows the TEM picture of a typical sample prepared using our vertical He-blowing method before acid treatment. The average particle size was found to be 33 ± 11 nm on the basis of measurements of over 50 nanoparticles. To remove the uncoated cobalt nanoparticles, the acid-treatment procedure described above was used. The corresponding TEM image is shown in Figure 2b. We found the average particle size to be 28 ± 9 nm. This suggests that the particle size did not change significantly after acid treatment. However, more amorphous carbon appeared as background after acid treatment (Figure 2b). A closer examination of the nanoparticles shows that most of these particles were normally coated by two or more graphite layers. It can also be seen in Figure 2b that some quasispherical pores were formed after acid treatment; these result from etching away of some partially coated cobalt particles by the acid. The

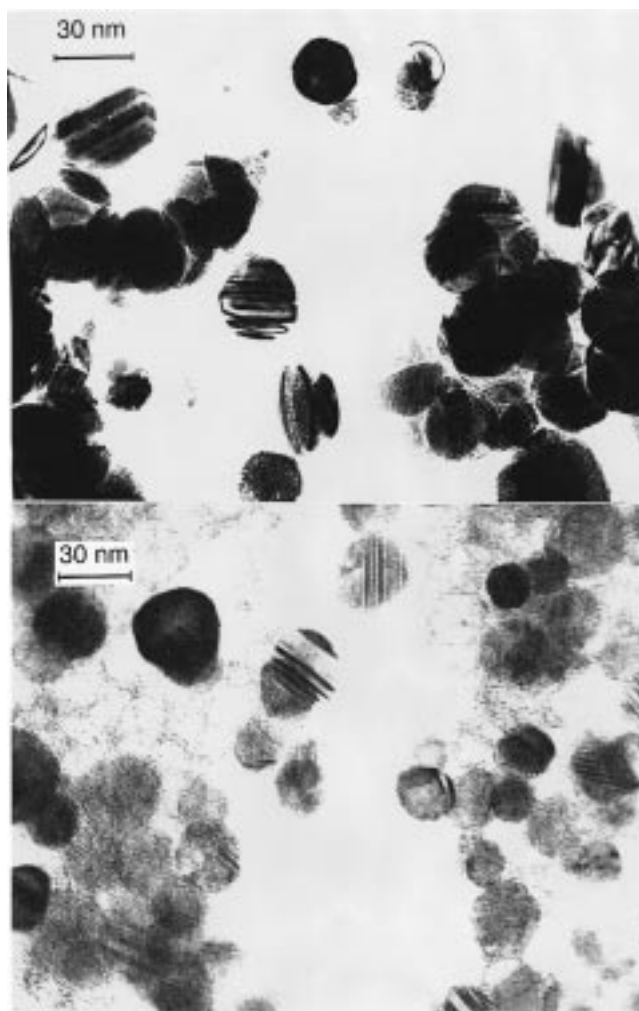


Figure 2. TEM images showing the morphologies of carbon-coated cobalt particles before (top) and after (bottom) acid treatment.

remaining weight percentage was normally between 40% and 70% and sometimes is as large as 85%. This is comparable with the results by Dravid et al. using a tungsten rod as the cathode.⁵

The growth morphology and the graphitization of the nanoparticle samples were sensitive to the discharge conditions such as the current density, the voltage, the dimension of the arcing gap, the buffer gas pressure, and the supply of carbon. Some of these factors were previously addressed experimentally (ref 5) and theoretically (ref 6) on the basis of the horizontal blowing scheme. We have investigated the influence of the speed of the quenching gas on the carbon-coated cobalt nanoparticles in our vertical gas-blowing setup. The most suitable speed of the gas was found to be between 0.5 and 5 m/s. The size of particles could be adjusted simply by changing the speed of the gas stream. Since the gas blew directly against the surface of the cobalt, the temperature of the cobalt, and hence the rate of cobalt evaporation, could be controlled by the blowing helium gas speed. Probably, the gas speed also determined the carbon supply from the graphite crucible since the gas stream was set between the crucible wall and the plasma region. When the gas speed was high (>6 m/s), giant Co particles as large as a few hundred nanometers were produced. These giant particles may be formed by the strong gas blow directly from the near-melted cobalt surface rather than from the plasma region. Alternatively, the cobalt nanoparticles may aggregate to form the giant particles owing to the reduced supply of carbon from

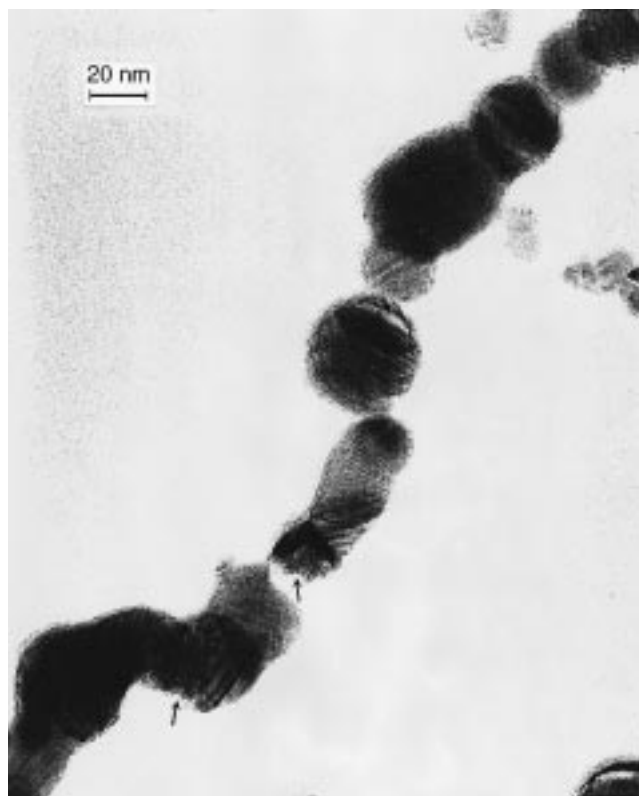


Figure 3. TEM image of chainlike carbon-coated cobalt particles formed when the blowing He gas speed was below 0.5 m/s. The arrows indicate the stacking faults of the cobalt particles.

the crucible wall. On the other hand, when the gas speed was low (<0.5 m/s), the carbon-coated cobalt particles aggregated in one dimension, forming chainlike particles. Figure 3 shows a chainlike agglomerate when the gas-blowing speed was below 0.5 m/s. Stacking faults of the cobalt particles can be seen as indicated by the arrows. The carbon shell around the cobalt particles became amorphous rather than graphitic. The cobalt particles could be separated very well when the gas speed was set between 0.5 and 5 m/s.

Shown in Figure 4 are the Raman spectra of the powder samples before and after acid treatment. The peak around 700 cm^{-1} in the spectrum of the sample before acid treatment is due to the uncoated cobalt as confirmed by the Raman spectra of the pure cobalt powder samples. After acid treatment, this peak around 700 cm^{-1} , associated with the uncoated cobalt, vanished, apparently owing to the fact that cobalt reacted readily with the acid.

In addition, several features regarding the effect of acid treatment on the Raman spectra are noteworthy. First, the intensities of the two first-order bands (1342 and 1582 cm^{-1}), attributable to the graphitic structures, increased dramatically. The 1582 cm^{-1} band is assigned to one of the two E_{2g} modes corresponding to the movement of two neighboring carbon atoms in opposite directions in a graphite sheet.⁷ The 1342 cm^{-1} band is normally explained by the relaxation of the wave vector selection rule resulting from the effect of the finite size of the crystal in the materials. This peak increases with an increase in the amount of disorganized carbon.⁸ The increased intensities of the two Raman peaks and their changed relative ratio after acid treatment then indicate that the content of the graphitic carbon component increases and the exposed cobalt particles are etched away. Second, it was observed, on the basis of a curve-fitting procedure, that after acid treatment the area ratio of the peak at $\sim 1583\text{ cm}^{-1}$ to that at 1342 cm^{-1} increased

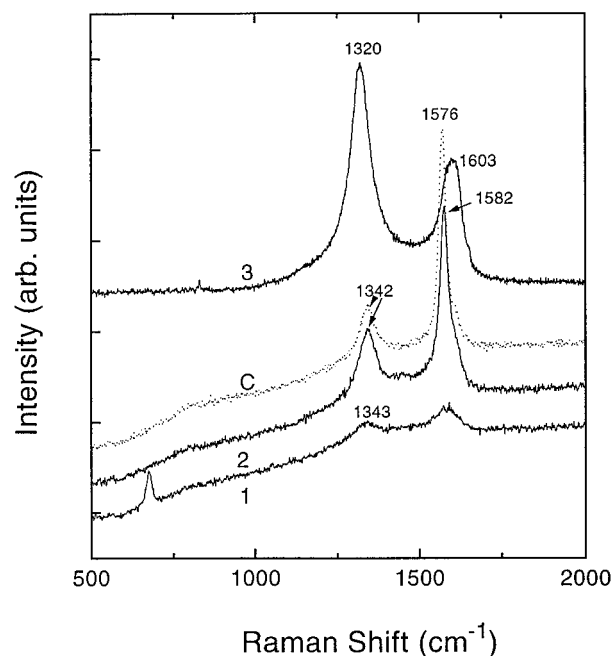


Figure 4. First-order Raman spectra of carbon-coated cobalt nanoparticle samples: (1) before acid treatment; (2) after acid treatment (for 1 week); (3) after acid treatment (for 5 months). The Raman spectrum of graphite powder ("c") is shown for reference.

by a factor of 1.5 to 3. This suggests that there are more "organized" carbon atoms exposed to the excitation laser beam. There are two possible reasons for this phenomenon. One is the additional graphitization caused by the heating of the sample through the exothermic process induced by the reaction between the uncoated or partially coated metal particles and the acid similar to the effect of annealing proposed by J. Jiao.⁹ Another reason is related to the assumption that the graphite-like layers initially imbedded by the cobalt aggregates became more easily exposed to the excitation laser beam for the Raman measurements after the acid etched away the unprotected cobalt metal particles. The heat from the reaction of the uncoated cobalt particles and the acid may be insufficient to promote the formation of graphitic layers since the temperature due to the reaction heat ($<80\text{ }^{\circ}\text{C}$) is well below the annealing temperature for the graphitic carbon materials ($>800\text{ }^{\circ}\text{C}$). As seen in the TEM pictures, the outermost parts of the carbon-coated particles are amorphous-like carbon while the inner parts are more graphite-like. The later explanation may be more reasonable, and it is also consistent with the inside-out graphite layer formation mechanism.⁶

Another feature of the Raman spectra is the peak shift after acid treatment. Compared with the Raman spectrum of pure graphite powder, the 1582 cm^{-1} peak shifts slightly upward (6 cm^{-1}) while the 1342 cm^{-1} peak does not show an observable shift. However, after aging in the acid for 5 months, dramatic shifts were observed for both Raman peaks. One is from 1582 to 1603 cm^{-1} and the other is from 1342 to 1320 cm^{-1} . The peaks also become broader. More interestingly, the peak intensities are reversed, which indicates that the carbon shell surrounding the cobalt nanoparticles becomes more disordered instead of exhibiting the expected acid catalytic graphitization effect. Fortunately, the cobalt domains are still coated by carbon as confirmed by TEM observations. Tests of these samples in magnetic fields showed that they are still strongly ferromagnetic, suggesting that the Co particles are well-protected by the carbon coating.

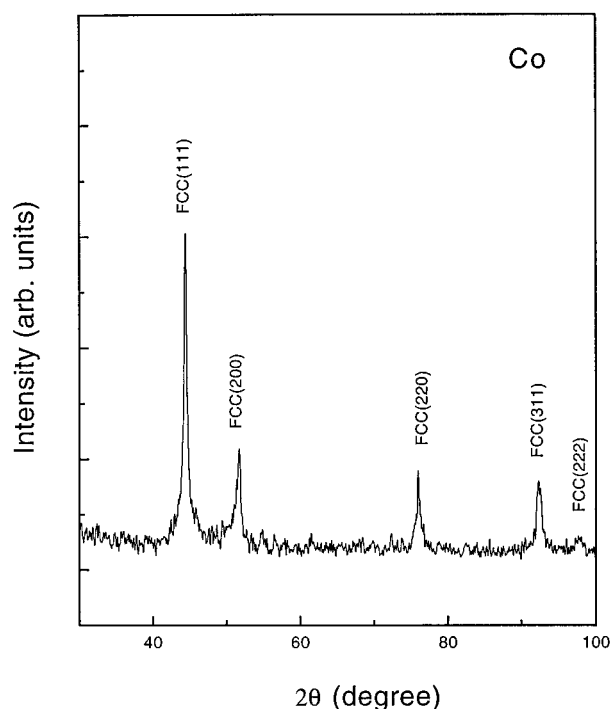


Figure 5. X-ray diffraction profile of carbon coated cobalt nanoparticles after acid treatment. Note that only the fcc structure can be identified.

It is well-known that cobalt exists in the fcc form at high temperatures, and it changes to the hcp structure at low temperatures. The transformation is sluggish so that the two forms coexist from room temperature up to 450 °C.¹⁰ As shown in Figure 5, however, only the fcc structure was observed by X-ray diffraction at room temperature. No hcp form and carbide phase were observed. This may be attributed to the fast quenching process.¹¹ However, we did not find any changes in the XRD pattern after cooling slowly (0.5 °C/min) from 600 °C down to room temperature under an Ar gas atmosphere. The fcc phase remains even after keeping the sample in liquid nitrogen for 3 days. We suggest that in the interface region between carbon and cobalt, some carbon atoms may occupy the octahedral cavities of the fcc structure of the cobalt domains, which would result in the difficulty of plane slipping from the fcc (ABCABC...) stacking to the hcp (ABAB...) stacking. An alternative explanation for the stability of the fcc face is related to the compression pressure felt by the Co crystallite lattice as a result of the small particle size as suggested by Dravid et al.⁵

The magnetization curve of the sample at room temperature is shown in Figure 6. The hysteresis loop demonstrates that the carbon-coated particles show soft ferromagnetic behavior at room temperature. The coercivity (H_c) and the saturation magnetization (M_s) of the sample (after acid treatment) are estimated to be 285 Oe and 88.5 emu/g, respectively. The ferromagnetic behavior of the sample is characterized by a ratio of the remnant-to-saturation magnetization expressed as M_r/M_s . For a typical carbon-coated cobalt nanoparticle sample we prepared, $M_r/M_s \sim 0.25$.

A very important property characteristic of magnetic nanoparticles is the blocking temperature (T_B), above which the ferromagnetic nanoparticles become superparamagnetic with zero coercivity ($H_c \rightarrow 0$). The smaller the nanoparticles, the easier the change of the magnetization directions, and consequently the lower the blocking temperature (T_B). Shown in the inset of Figure 6 is a thermogravimetric curve of the sample measured under a magnetic field gradient and a N₂ atmosphere.

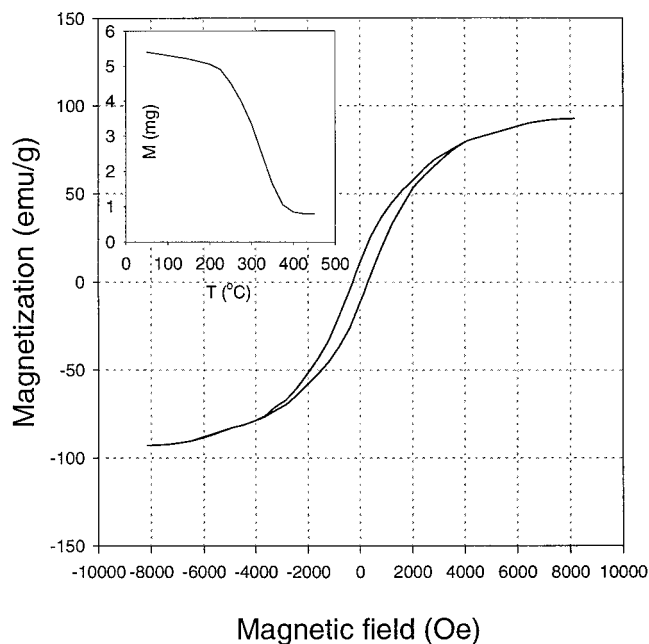


Figure 6. Plot of magnetization versus magnetic field for a typical carbon-coated cobalt nanoparticle sample (~30 nm) after acid treatment at room temperature. The inset is a thermogravimetric (TG) curve under a magnetic field gradient for the measurement of the blocking temperature (T_B).

The blocking temperature (T_B) is estimated to be 373 °C from this curve. This is, to our knowledge, the first direct measurement of the blocking temperature of the carbon-coated cobalt nanoparticles. The blocking temperature we obtained is well above room temperature and much higher than the corresponding value for the sample ($T_B = 160$ K, $r \sim 3.9$ nm) prepared by M. E. McHenry's group.² The sizes of our particles ($r \sim 15$ nm) are larger than those of McHenry's sample ($r \sim 3.9$ nm), so a higher blocking temperature is expected. In addition, the technique we used to estimate the blocking temperature is different from that used by McHenry et al., and this could also contribute to the difference in the blocking temperatures estimated by the two groups. According to the theory of superparamagnetism, the blocking temperature T_B should roughly satisfy the relationship:

$$\tau = \tau_0 e^{[K \cdot V / (k_B \cdot T_B)]}$$

where τ is the time scale (several minutes) of the experimental measurement of the magnetic properties of the nanoparticles; τ_0 is on the order of 10^{-10} and 10^{-12} s. k_B is the Boltzmann constant. For the fcc Co at 0 K, $K = -2.7 \times 10^6$ erg/cm³, and τ_0 is around 10^{-11} s.¹² By substituting these values into the above equation, we obtain the average volume of $\langle V \rangle \sim 4.2 \times 10^{-24}$ m³, which corresponds to a mean particle radius of $r \sim 15$ nm. This is in good agreement with our TEM observations shown in Figure 2.

Summary and Conclusions

In summary, a modified arc-discharge setup coupled with an internal and vertical gas-blowing scheme has been successfully used to prepare carbon-coated cobalt nanocrystals. This was shown to be an efficient method to prepare uniform carbon-coated cobalt nanoparticles. Large Raman peak shifts were observed for these carbon-coated cobalt nanoparticles upon acid treatments, which are ascribed to the changed carbon structures induced by the acid treatments. The blocking temperature of

the carbon-coated nanoparticles was found to be 373 °C with a vibrating sample magnetometer and a thermogravimetric analyzer in a magnetic field gradient. This blocking temperature is well above room temperature, which reflects the relatively large size of these nanoparticles.

Acknowledgment. This work was supported by an RGC Grant (HKUST6150/97P) administered by the UGC of Hong Kong. The assistance and suggestions of Dr. Supapan Seraphin for our initial work are greatly appreciated. The authors thank the staff of MCPF at HKUST, particularly Mr. Jiaqi Zheng and Mr. Keith Moulding for their kind help in sample characterization. Thanks are given to Dr. Richard Haynes for proofreading the original manuscript.

References and Notes

- (1) Majetich, A.; Artman, J. O.; McHenry, M. E.; Nuhfer, N. T.; Staley, S. W. *Phys. Rev. B* **1993**, *48*, 16845.
- (2) McHenry, M. E.; Majetich, S. A.; Artman, J. O.; DeGraef, M.; Staley, S. W. *Phys. Rev. B* **1994**, *49*, 11358. McHenry, M. E.; Majetich, S. A.; Kirkpatrick, E. M. *Mater. Sci. Eng. A* **1995**, *204*, 19.
- (3) Hihara, T.; Onodera, H.; Sumiyama, K.; Suzuki, K.; Kasuya, A.; Nishina, Y.; Saito, Y.; Yoshikawa, T.; Okuda, M. *Jpn. J. Appl. Phys.* **1994**, *33*, L24. Saito, Y.; Yoshikawa, T.; Okuda, M.; Fujimoto, N.; Yamamuro, S.; Wakoh, K.; Sumiyama, K.; Suzuki, K.; Kasuya, A. *J. Appl. Phys.* **1994**, *75*, 134. Saito, Y.; Masuda, M. *Jpn. J. Appl. Phys.* **1995**, *34*, 5594. Saito, Y. *Carbon* **1995**, *33*, 979. Saito, Y.; Ma, J.; Nakashima, J.; Masuda, M. *Z. Phys. D* **1997**, *40*, 170.
- (4) Seraphin, S.; Wang, S.; Zhou, D.; Jiao, J. *Chem. Phys. Lett.* **1995**, *228*, 506. Seraphin, S. *J. Electrochem. Soc.* **1995**, *142*, 290. Jiao, J.; Seraphin, S.; Wang, X. K.; Withers, J. C. *J. Appl. Phys.* **1996**, *80*, 103. Seraphin, S.; Zhou, D.; Jiao, J. *J. Appl. Phys.* **1997**, *80*, 2097.
- (5) Dravid, V. P.; Host, J. J.; Teng, M. J.; Elliott, B.; Hwang, J.; Johnson, D. L.; Mason, T. O.; Weertman, J. R. *Nature* **1995**, *374*, 602. Host, J. J.; Teng, M. J.; Elliott, B.; Hwang, J.; Mason, T. O.; Johnson, D. L.; Dravid, V. P. *J. Mater. Res.* **1997**, *12*, 1268.
- (6) Elliott, B. R.; Host, J. J.; Dravid, V. P.; Teng, M. H.; Hwang, J. H. *J. Mater. Res.* **1997**, *12*, 3328.
- (7) Ebbesen, T. W. *Carbon Nanotube: Preparation and Properties*; CRC Press Inc.: Boca Raton, FL, 1997, p 228.
- (8) Kinoshita, K. *Carbon: Electrochemical and Physicochemical Properties*; John Wiley & Sons: New York, 1988; p117.
- (9) Jiao, J.; Seraphin, S. 189th Meeting of the Electrochemical Society, 1996.
- (10) Lupis, C. H. P. *Chemical Thermodynamics of materials*; North-Holland: New York, 1983; p 367.
- (11) Jiao, J. Comparative Study of the Properties, Morphologies and Structures of Carbon Nanoclusters Prepared by Different Methods. Ph.D. Dissertation, 1997.
- (12) Sucksmith, W. A.; Thompson, J. E. *Proc. R. Soc. London Ser. A* **1954**, *225*, 362.